Modulating Electronic Transport Properties of Carbon Nanotubes To Improve the Thermoelectric Power Factor *via* Nanoparticle Decoration

Choongho Yu,[†,‡,*] Yeontack Ryu,[†] Liang Yin,[†] and Hongjoo Yang[†]

[†]Mechanical Engineering Department and [‡]Materials Science and Engineering, Texas A&M University, College Station, Texas 77843, United States

ABSTRACT Nanoparticle decoration on carbon nanotubes was employed to modulate their electrical conductance and thermopower and thereby improved the thermoelectric power factor. Nanotubes were made into films by spraying nanotube solutions on glass substrates, and then the films were immersed in different concentrations of $CuSO_4$ or $HAuCl_4$ solutions for various time periods. Copper ions in the solutions were reduced on nanotubes by obtaining electrons from zinc electrodes, whose reduction potential is lower than that of copper (galvanic displacement). Gold ions were reduced on nanotubes by both silver counter electrodes and spontaneous reaction due to larger reduction potentials than those of nanotubes. These reactions made electrons donated to (copper incorporation) or withdrawn from (gold incorporation) nanotubes depending on the difference in their work functions and reduction potentials, resulting in considerable changes in electron transport. In this paper, a series of experiments at different ion concentrations and reaction time periods were systematically performed in order to find optimum nanoparticle formation conditions and corresponding electronic transport changes for better thermoelectric power factor. Transport measurement results show that electronic properties can be considerably altered and modulated, resulting in 2-fold improvement in the thermoelectric power factor with 1 mM/30 min reaction. Reactions with solutions of a low metal ion concentration, such as 1 mM, yielded well-distributed small particles over large surface areas, which strongly affected electron transfer between nanoparticles and nanotubes. Successive copper and gold decorations on nanotubes made electrical conductance (or thermopower) serially decreased and increased (or increased and decreased) upon precipitating different metal particles. This transport behavior is believed to be from the changes in the Fermi level as a result of electron exchanges between reduced metals and nanotubes. Thermopower improvement after copper decoration can be attributed to the enlarged gap between the Fermi level and the mean of differential electrical conductivity. Such behaviors often appear when the Fermi level is shifted toward the spike-shape density of states in nanotubes due to anisotropic differential electrical conductivity. Finally, this study demonstrates that the thermoelectric power factor can be considerably increased by properly locating the Fermi level of carbon nanotubes with nanoparticles, providing promising opportunities of developing efficient organic thermoelectric materials as well as various electronic materials of desired properties.

KEYWORDS: nanoparticle decoration · carbon nanotube · thermoelectric · power factor · electrical conductivity · thermopower · Seebeck coefficient

Carbon nanotubes have excellent intrinsic electrical properties, which are very promising for many applications including thermoelectrics,[1−4] nanoelectronics,[5] and photovoltaics.[6,7] Furthermore, they are very sensitive to external disturbances, making them ideal for sensing tiny species.[8] Furthermore, when nanotubes are made into films or bulk materials, junctions between nanotubes can be modified to obtain desired electrical and thermal transport properties.[1] Such dramatic changes are caused by their unique carrier transport characteristics along a sheet of graphite in a cylindrical shape. The unique transport characteristics provide great opportunities for manipulating electronic transport properties. For instance, this is essential to synthesizing efficient thermoelectric materials, which require high electrical conductivity and thermopower (or the Seebeck coefficient) with low thermal conductivity. A measure of thermoelectric efficiency (Z) is often described as $Z = S^2\sigma/k$, where S, σ, and k, respectively, are thermopower, electrical conductivity, and thermal conductivity.[9] In typical bulk materials, strong correlations between these parameters make Z improvement extremely difficult. For example, an increase of σ hampers S, resulting in a small change of $S^2\sigma$ (called as the power factor). In general, in order to achieve a large power factor, it is necessary to have a large anisotropy such as narrow sharp bands in the electronic density of states.[10] Carbon nanotubes whose electronic density of states has spike-shape Van Hove singularities are excellent for this purpose. The Fermi level of nanotubes can be readily altered by using impurities such as nanoparticles and molecules. In this paper, nanoparticle precipitations on nanotubes were performed by using galvanic displacement or the difference of reduction potentials between nanotubes and reducing agents.[11,12] In case of galvanic displacement, metal ions in a solution were reduced on nanotubes by dissolving another metal whose reduction potential is smaller than that of the reduced metal. Electrons released from the dissolved metal are delivered to the ions in

*Address correspondence to chyu@tamu.edu.

Received for review November 5, 2010 and accepted January 3, 2011.

Published online January 11, 2011
10.1021/nn102999h

the solution, forming metal nanoparticles on nanotubes. When the reduction potential of ions in a solution is larger than that of nanotubes, nanoparticles are also spontaneously precipitated. The spontaneous reduction method is limited to a few metals such as gold and platinum, whereas the galvanic displacement method can be used for obtaining various metal nanoparticles. Charge transfers between nanoparticles and nanotubes as well as structural changes due to particle incorporations may considerably alter transport properties due to modifications of carrier densities, mobilities, and contact junctions. In this study, 200% increases in the thermoelectric power factor were observed with copper nanoparticle decorations on nanotubes. Methodologies of manipulating thermopower/electrical conductivity as well as morphologies/structures of nanoparticles upon various reaction conditions were also presented. A series of experiments at different ion concentrations and reaction time periods were systematically performed in order to find nanoparticle formation conditions that improve the thermoelectric power factor. The following describes experimental procedures, electronic properties upon decorating various density and size nanoparticles on nanotubes, as well as a discussion regarding transport property changes.

RESULTS AND DISCUSSION

Nanotubes were fabricated into films by spraying nanotubes dispersed by sodium dodecyl benzene sulfonate (SDBS) in deionized water. The films were immersed in solutions with different copper or gold ion concentrations for various time periods in order to precipitate nanoparticles of different sizes and densities. In order to attach copper or gold nanoparticles to nanotubes, either zinc or silver electrodes were used for galvanic displacement. Gold reduction potential ($[AuCl_4]^- + 3e^- \rightarrow Au(s) + 4Cl^-$, standard electrode potential (E^0) = +0.93 V)[13] is larger than silver ($Ag^+ + e^- \rightarrow Ag(s)$, E^0 = +0.7996 V),[13] making gold ions reduced on nanotubes by ionizing silver. Copper reduction potential ($Cu^{2+} + 2e^- \rightarrow Cu(s)$, E^0 = +0.34 V)[13] is close to E^0 (+0.2 to +0.5 V)[14,15] of carbon nanotubes but is much larger than that of zinc ($Zn^{2+} + 2e^- \rightarrow Zn(s)$, E^0 = −0.7618 V).[13] Note that the Fermi level of nanotubes is typically measured in vacuum environment), but it does change depending on doping (*i.e.,* oxygen doping when nanotubes are exposed to air[16]). The samples were immersed in aqueous solutions of 1, 10, and 20 mM $CuSO_4$ for 30 s, 3 min, 10 min, 15 min, 30 min, 1 h 30 min, 3 h, or 18 h. Scanning electron micrographs (SEMs) are shown in Figure 1 after 30 s (Figure 1a1−c1), 3 min (Figure 1a2,b2), 15 min (Figure 1c2), or 30 min (Figure 1a3−c3) reactions. Nanoparticles start to precipitates even with the lowest concentration (1 mM) for 30 s (Figure 1a1). Particle sizes range from a few nanometers to a hundred nanometers

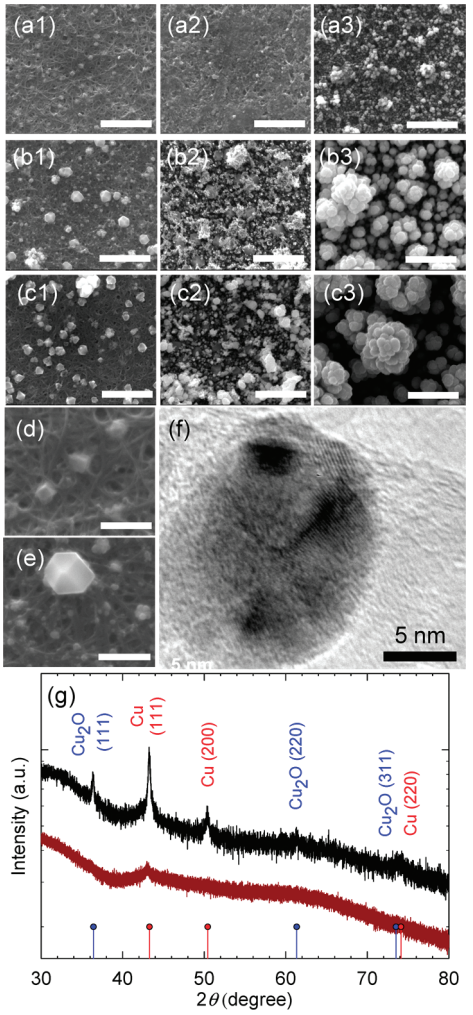

Figure 1. Nanotube films after reactions in $CuSO_4$ solutions of the following concentrations for various time periods: (a1) 1 mM/30 s, (a2) 1 mM/3 min, (a3) 1 mM/30 min, (b1) 10 mM/30 s, (b2) 10 mM/3 min, (b3) 10 mM/30 min, (c1) 20 mM/30 s, (c2) 20 mM/15 min, (c3) 20 mM/30 min, (d) a portion of (a1) with a higher magnification, (e) a portion of (b1) with a higher magnification, (f) copper nanoparticle (ellipse at the center) attached to nanotube bundles (wavy lines in the horizontal direction), and (g) X-ray diffractions of the sample shown in (b2) (upper black line) and (a3) (lower brown line). The scale bars for (a1)−(c3) represent 2 μm, and those for (d) and (e) are 500 nm. Smaller nanoparticles were precipitated after reactions with the low concentration solutions, which provide more surface areas for a given volume of materials.

(see the image with a 500 nm scale bar in Figure 1d). As the reaction time was increased to 3 min (Figure 1a2) and 30 min (Figure 1a3), the size and density of particles were increased. Low ion concentration resulted in slow particle precipitation rates compared to those with high concentrations (compare the 1 mM case (Figure 1a1) with 10 mM (Figure 1b1) for 30 s reactions; compare the 1 mM case (Figure 1a2) with 10 mM (Figure 1b2) for 3 min reactions). When high concentration solutions (10 and 20 mM) were used, copper nanoparticles coalesced, resulting in relatively large (a few hundred nanometers) particles. The particles from a high concentration

(20 mM) clearly show crystalline faces, as indicated in Figure 1e. Images in Figure 1a3,b2, respectively, from 1 mM/30 min and 10 mM/3 min reactions indicate that a lower concentration makes less dense and smaller nanoparticles. A long period reaction with a high concentration such as 20 mM/30 min reaction in Figure 1c3 formed a continuous layer of nanoparticles. A transmission electron micrograph of a sample with a 1 mM/30 min copper reaction shows crystalline nanoparticles attached to nanotube bundles, as shown in Figure 1f. Lattice patterns are shown in the particle (dark ellipse), and nanotube bundles are shown as wavy lines in the horizontal direction. X-ray diffraction patterns of samples (Figure 1g) after 1 mM/30 min (lower plot, brown color) and 10 mM/3 min (upper plot, black color) reactions indicate that the reaction with a higher concentration is easier to crystallize copper than that with a lower concentration. The crystalline Cu_2O may have formed during the experiments since the sample was exposed to water and air. In general, O_2 dissolved in the water-based solution is dissociated upon reaction with copper and then forms Cu_2O unless the reaction occurs at high temperatures.[17,18] Since the oxidation process does not involve charge transfer between nanotubes and copper (or Cu_2O), the oxidation is not likely to have significant influence on changing carrier concentrations in nanotubes.

Electrical conductance and thermopower measurement results are plotted in Figure 2a,b, and the power factors were calculated (Figure 2c). All properties were normalized by those of samples prior to metal decoration processes. Note that the initial conductance/thermopower as well as film thicknesses (150−200 nm) were similar. In addition, metal ions can access nanotubes located at both outer and inner parts of the films due to numerous voids between tangled nanotubes (see micrographs in Figure 1). For 1 and 10 mM reactions, the electrical conductance was decreased with increasing reaction time. On the contrary, the reaction with 20 mM for 30 min suddenly doubled conductance. This is because the dense copper particles, shown in Figure 1c3, are likely to be electrically connected. The electrical conductivity of bulk copper ($\sim 6 \times 10^7$ S/m at 300 K)[19] is typically 1 or 2 orders higher than those of carbon nanotube films. Note that the intrinsic electrical conductivity of nanotubes is up to $\sim 2 \times 10^7$ S/m at room temperature,[20] but electron transport is hampered by contact resistance between nanotubes in films and bulk materials. Electrical conductivity and thermopower of as-synthesized films in this study are measured to be $5 \times 10^4 \sim 10^5$ S/m and 25−30 μV/K at 300 K. The significant reduction from 1 to 0.64 for the normalized thermopower after a 20 mM−30 min reaction (blue square, shown in Figure 2b) would imply that copper has participated in electron transport. Note that the thermopower of copper is small (1.83 μV/K at 300 K).[9] On the other hand, thermopower after 1 mM

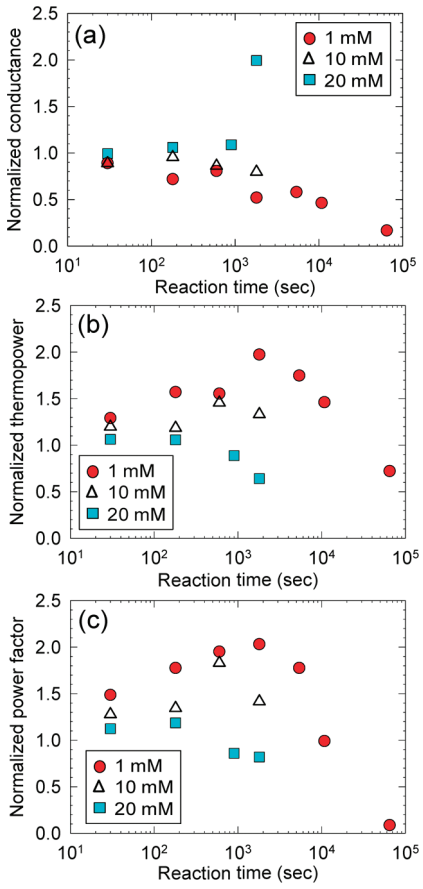

Figure 2. Normalized conductance (a), thermopower (b), and the power factor (c) after reactions in 1, 10, and 20 mM $CuSO_4$ solutions as a function of reaction time. Reactions in 1 mM solution resulted in 200% increase of the power factor.

reactions was progressively increased as a function of reaction time but decreased with reaction times longer than 30 min. The increase of thermopower yielded a large enhancement in the power factor up to 200%, as shown in Figure 1c. These results indicate that it is better to use low ion concentrations to maintain the small size of the particles. Smaller particles have more surface areas for given volumes and are likely to provide more sites for charge interactions without forming thick continuous metal layers.

In order to study transport behaviors upon changing materials, gold nanoparticles were incorporated on nanotubes, as shown in Figure 3. Nanoparticles were precipitated by immersing nanotube films in a 1 mM $HAuCl_4$ solution for 30 s (Figure 3a), 15 min (Figure 3b), and 120 min (Figure 3c). The large particles are composed of small ones, which indicates that the size of individual particles is a few tens of nanometers or less. Gold particles were synthesized by spontaneous gold reduction as well as galvanic displacement of silver electrodes deposited on nanotube films. The galvanic displacement was observed to be stronger than the spontaneous reduction. Without silver electrodes, gold reduction was slow, leaving only a small density of nanoparticles on samples. We noticed that gold

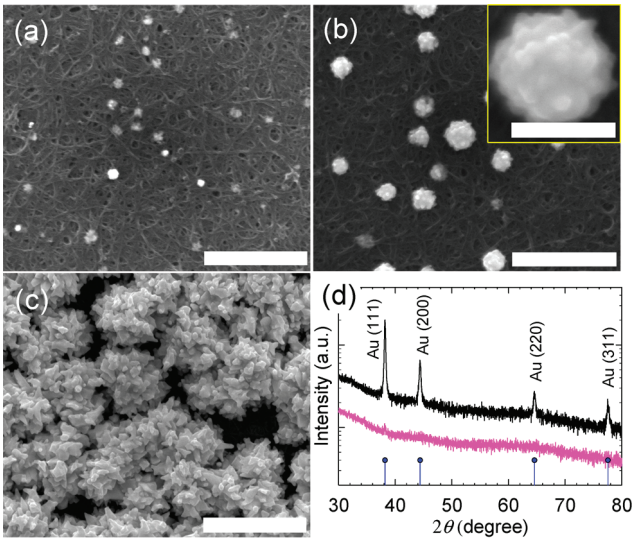

Figure 3. Nanotube films reacted in 1 mM $HAuCl_4$ solutions for (a) 30 s, (b) 15 min, and (c) 120 min. The scale bars represent 2 μm, and the inset scale bar is 500 nm. (d) X-ray diffractions of the samples shown in (a) (lower pink line) and (c) (upper black line). Gold nanoparticles precipitated on the sites that particles were created, forming bigger particles when reaction time was increased.

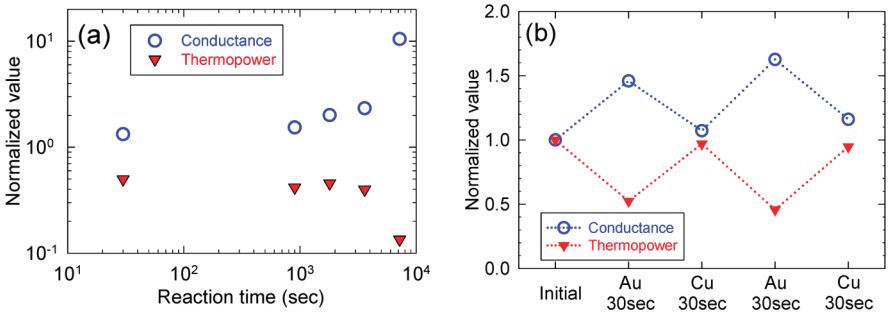

Figure 4. (a) Normalized conductance (blue circles) and thermopower (red triangles) as a function of reaction time after reactions in 1 mM $HAuCl_4$ solutions. (b) Normalized conductance (blue circles) and thermopower (red triangles) after two successive 30 s reactions in a 1 mM $HAuCl_4$ solution followed by a 1 mM $CuSO_4$ solution.

reduction could be facilitated when samples were made of nitric acid treated nanotubes (reflux in 70% HNO_3 for several hours). Presumably, functionalized and/or defective nanotube surfaces created by the acid treatment are helpful in the reduction processes. Note that samples in this study were made of purified-grade nanotubes without additional treatments, and nanotubes contain 4−7% metal (Ni, Y) impurities according to manufacturer's product information. The X-ray diffraction from a 120 min reaction (upper plot, black line in Figure 3d) clearly indicates the presence of crystalline gold, but the weak peaks from a 30 s reaction (lower plot, pink line in Figure 3d) might be due to the small density, size, and/or amorphous structures of the particles.

The gold incorporation increased conductance of all samples with reductions in thermopower (see Figure 4a). With a long reaction (120 min) in a 1 mM $HAuCl_4$ solution, the conductance was boosted by 1 order of magnitude. This large increase is likely to be from electrically conducting paths along dense gold particles shown in Figure 3c. Conductance and thermopower were measured when nanotube films were immersed in two different solutions (a 1 mM $HAuCl_4$ solution followed by a 1 mM $CuSO_4$ solution for 30 s each) in series. Figure 4b indicates that the changes in electrical conductance and thermopower were reversible when gold and copper were serially incorporated on nanotubes. Upon the gold incorporation, conductance was increased with a reduction of thermopower, and the copper incorporation resulted in the opposite behaviors.

The reversible change in electronic transport properties occurs when electrons are readily transferred from metals to nanotubes or *vice versa* depending on the work function of metals relative to those of nanotubes. When metals are precipitated, the difference between their Fermi levels at metal−nanotube contacts induces electron transfer to equilibrate the Fermi levels. The work functions of copper, gold, and nanotubes are, respectively, 4.38−4.65,[21,22] 5.0−5.22,[22] and 4.7−5.0 eV.[14,15] Hence, when copper is in contact with nanotubes, electrons are donated to nanotubes, making them more n-type materials. On the other hand, gold incorporation makes nanotubes more p-type by

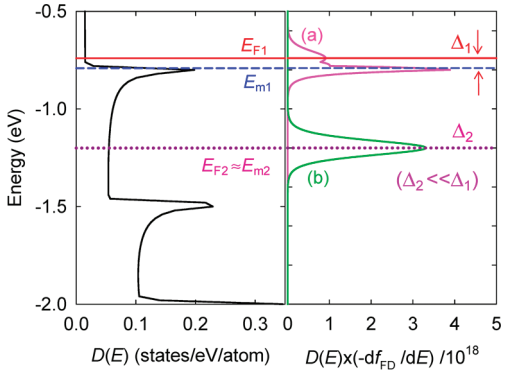

Figure 5. (Left) Electronic density of states ($D(E)$) for a single-walled carbon nanotube with (10,10) chirality. (Right) Energy against $D(E)(-\partial f_{FD}/\partial E)$ that is proportional to the differential electrical conductivity (ψ in eq 1). (a) $D(E)(-\partial f_{FD}/\partial E)$ when the Fermi level, E_{F1}, is near the spike-shape density of states (pink line). The gap (Δ_1) between E_{F1} and E_{m1} is relatively large, increasing the magnitude of thermopower ($|S|$). (b) $D(E)(-\partial f_{FD}/\partial E)$ when the Fermi level, E_{F2}, is near the flat density of states (green line). The gap (Δ_2) between E_{F2} and E_{m2} is very small, leading to small thermopower.

withdrawing electrons from nanotubes. When gold particles are spontaneously precipitated, electrons are transferred from nanotubes to gold ions. Nanotubes have shallow density of states near the Fermi level, and small changes in carrier density are likely to alter the Fermi level of nanotubes significantly. The shift of the Fermi level may give rise to a large change in thermopower with small changes in electrical conductivity. When the Fermi level is located near the spike in the density of states of nanotubes, such changes of thermopower would result in a net increase of the power factor such as the case of the 1 mM/30 min copper reaction shown in Figure 2c. Let us recall electrical conductivity (σ) and thermopower (S):[23]

$$\sigma = \int \psi(E)\mathrm{d}E;\ \psi(E) \sim D(E)(-\partial f_{FD}/\partial E) \quad (1)$$

$$S = -\frac{1}{eT}\frac{\int \psi(E)(E-E_f)\mathrm{d}E}{\int \psi(E)\mathrm{d}E};\ |S| \sim \frac{|E_m - E_f|}{eT} \equiv \frac{\Delta}{eT} \quad (2)$$

Here, E and E_f are energy and the Fermi level; $D(E)$ and f_{FD} are the electronic density of states and the Fermi–Dirac distribution; e and T are electron charge and temperature; Δ is the energy gap between mean energy (E_m) of the differential electrical conductivity ($\psi(E)$) and the Fermi level, E_f. Electrical conductivity can be represented by the area under the differential electrical conductivity since it is obtained by integrating $\psi(E)$ from the definition in eq 1. In order to obtain a large thermopower, it is necessary to increase Δ (see eq 2), which can be obtained by making the shape of $\psi(E)$ anisotropic. This behavior is conceptually described in Figure 5 with a metallic nanotube of (10,10) chirality. The density of states (black solid line in Figure 5 left pane) was calculated by the local density approximation of density functional theory.[24] When electrons are injected "to" nanotubes by copper incorporation, the Fermi level is located at an energy level higher than that of nanotubes decorated by gold (electrons are withdrawn "from" nanotubes). For example, the red solid (E_{F1}) and purple dotted (E_{F2}) lines may represent the Fermi levels after copper and gold reactions, respectively. Figure 5a,b represents $D(E)$-$(-\partial f_{FD}/\partial E)$, which is proportional to the differential electrical conductivity (ψ in eq 1), for the samples after (a) copper and (b) gold reactions, respectively. When the Fermi level of nanotubes is located near the energy level where the density of states has a spike-like shape (*e.g.*, E_{F1}), the differential electrical conductivity becomes anisotropic (see the pink solid line in Figure 5a). This enlarges the energy gap, Δ_1 ($\equiv|E_{m1}-E_{F1}|$), that is proportional to the magnitude of thermopower. When n-doping is so strong that the Fermi level is raised well above E_{F1} toward the flat regime, the differential electrical conductivity becomes symmetric, decreasing the magnitude of thermopower. This behavior was observed when reaction time is longer than 1 mM/30 min, as shown in Figure 2b. Note that this is not likely from the small thermopower of copper because conductance was monotonically decreased with increasing reaction time. In other words, the 1 mM concentration is too low to form continuous copper films within the time period of our experiments, resulting in a monotonic reduction of hole concentrations in nanotubes. If copper nanoparticles were connected to each other, conductance would have been considerably increased such as the experiment with the 20 mM/30 min condition (see blue squares in Figure 2a). On the contrary, when nanotubes become more p-type and the Fermi level is located near a flat regime of the density of states, the shape of the differential electrical conductivity is symmetric, resulting in small Δ_2 ($\equiv|E_{m2}-E_{F2}|$) (see the green solid line in Figure 5b). When nanotubes were additionally doped with oxygen by annealing samples in a tube furnace at 250 °C with 10 sccm oxygen flow for 3 h, thermopower was further increased. This is likely from additional p-type doping that lowers the Fermi level close to another spike in the density of states. Upon vacuum annealing at $\sim 10^{-8}$ Torr at 250 °C for 3 h, thermopower was decreased likely due to oxygen desorption.

CONCLUSIONS

In summary, nanoparticle incorporation on nanotubes modulated electrical conductance and thermopower of nanotube films, raising their thermoelectric power factors. Nanotubes were made into films by spraying nanotube solutions on glass substrates. Then, copper or gold ions were reduced by immersing the films into $CuSO_4$ or $HAuCl_4$ solution of different concentrations for various time periods. Copper was precipitated by using zinc electrodes whose reduction potential is lower than that of copper. Gold reduction

was facilitated by silver counter electrodes, but at the same time, gold was also spontaneously reduced on nanotubes due to the larger reduction potential of gold than those of nanotubes. Reactions in low ion concentration solutions generated small (a few tens of nanometers) particles, while particles coalesced during ion reduction in high concentration solutions. In the case of copper incorporation, electrons were believed to be donated to nanotubes (more n-type). Gold reduction takes electrons from nanotubes, making samples more p-type. A series of experiments at different ion concentrations and reaction time periods were systematically performed in order to reveal nanoparticle formation conditions and electronic transport changes that improve the thermoelectric power factor. The experimental results show the transport properties can be considerably altered and modulated, resulting in 2-fold improvement in the thermoelectric power factor with a 1 mM/30 min reaction. Reactions in low ion concentration solutions yielded well-distributed small particles, which provided large surface areas and thereby strongly affected electrical properties of nanotubes. It has also been found that electrical property changes are reversible. Successive copper and gold decorations on nanotubes made electrical conductance (or thermopower) serially decreased and increased (or increased and decreased). These transport behaviors are believed to be from the modification of the Fermi level as a result of electron exchanges between reduced metals and nanotubes. Upon nanoparticle precipitation, electron transfer occurs in order to equilibrate the Fermi levels of materials in contact. Additionally, tube−tube junctions may have been modified as a result of bridging nanotubes with nanoparticles. The thermopower enhancement after copper decoration can be attributed to the enlarged gap between the Fermi level and the mean of differential electrical conductivity. Such behaviors often appear when the Fermi level is shifted toward the spike-shape density of states in nanotubes due to anisotropic differential electrical conductivity. Electrical conductance was improved when carrier concentrations were raised as a result of nanoparticle precipitation.

METHODS

Twelve milligram carbon nanotubes (purified grade nanotubes synthesized by arc discharge method; P2-SWNT, Carbon Solution Inc.) were dispersed in 20 mL of deionized (DI) water with 24 mg of sodium dodecyl benzene sulfonate (SDBS, Acros organics, 88%) by ultrasonication for 3 min. Then, the solution was centrifuged at 6000 rpm for 15 min in order to obtain supernatant solution. According to the product information of P2-SWNT, metal contents (Ni, Y) range from 4 to 7 wt % and carbonaceous purity is greater than 90%. Average diameters of individual tubes and bundles are 1.4 and 4−5 nm, respectively. The average length of bundles ranges from 500 nm to 1.5 μm. The solution was sprayed on glass slides at a temperature of ~80 °C with a spray gun (Fuso Seiki Co., GP-S1, 0.2 mm nozzle diameter). The thickness of samples was strongly dependent on solution quantity, which was kept the same for all samples in this study. Typical film thicknesses were measured to be 150−200 nm. Then, the samples were immersed into deionized water for 30 min to remove SDBS surfactant and subsequently dried by compressed air. The typical size of samples is ~6 mm × 25 mm. Metal ion solutions were prepared by dissolving $CuSO_4$ (Fisher Scientific, 99+%) and $HAuCl_4$ (Alfa Aesar, 99.9%) in deionized water. The samples were immersed into 1, 10, or 20 mM concentration solutions for various time periods. Thin electrodes made of a silver paint at the end of the long edge of the samples were used for gold incorporation. Zinc foils were attached to the electrodes of nanotube films by a silver paint for copper incorporation.

Electrical conductance and thermopower were measured at room temperature by using a homemade four-probe setup with two T-type thermocouples and two copper wires. Four silver line shape electrodes were made on both edges of the samples for the measurements. Then, the samples were placed on a setup that was composed of two thermoelectric devices to create variable temperature difference. A current−voltage (I−V) sweeping method across the long edge of the samples was employed to generate linear I−V curves to obtain sample conductance. Voltages between two electrodes at both ends of the samples were measured at six different temperature differences between 0 and ±7 °C to extract thermopower. The transport properties were characterized before and after nanoparticle incorporation processes. Film thicknesses were measured by using an optical surface profilometer (Wyko NT9100 optical profiler, Veeco Instruments Inc.). Morphology, structure, and energy-dispersive spectroscopy analyses were performed by using a SEM (Quanta 600), a TEM (JEOL JEM-2010), and an X-ray diffractometer (Bruker-AXS D8 VARIO).

Acknowledgment. The authors gratefully acknowledge financial support from the U.S. Air Force Office of Scientific Research (Grant No. FA9550-09-1-0609) under the auspices of Dr. Charles Lee, the U.S. National Science Foundation (Grant No. CMMI 1030958), and the Pioneer Research Center Program through the National Research Foundation of Korea (Grant No. 2010-0002231) funded by the Ministry of Education, Science and Technology (MEST).

Note Added After Asap Publication. Due to a production error, the version of this paper that was published online January 11, 2011, mistakenly identified the third author as a corresponding author. This error was corrected and the revised version was published January 26, 2011.

REFERENCES AND NOTES

1. Yu, C.; Kim, Y. S.; Kim, D.; Grunlan, J. C. Thermoelectric Behavior of Segregated-Network Polymer Nanocomposites. *Nano Lett.* **2008,** *8*, 4428–4432.
2. Kim, D.; Kim, Y.; Choi, K.; Grunlan, J. C.; Yu, C. Improved Thermoelectric Behavior of Nanotube-Filled Polymer Composites with Poly(3,4-ethylenedioxythiophene)−Poly(styrenesulfonate). *ACS Nano* **2010,** *4*, 513–523.
3. Kim, Y. S.; Kim, D.; Martin, K. J.; Yu, C.; Grunlan, J. C. Influence of Stabilizer Concentration on Transport Behavior and Thermopower of Carbon Nanotube Filled Latex-Based Composites. *Macromol. Mater. Eng.* **2010,** *295*, 431–436.
4. Yu, C.; Shi, L.; Yao, Z.; Li, D.; Majumdar, A. Thermal Conductance and Thermopower of an Individual Single-Wall Carbon Nanotube. *Nano Lett.* **2005,** *5*, 1842–1846.
5. Appenzeller, J. Carbon Nanotubes for High-Performance Electronics—Progress and Prospect. *Proc. IEEE* **2008,** *96*, 201–211.
6. Wu, Z. C.; Chen, Z. H.; Du, X.; Logan, J. M.; Sippel, J.; Nikolou, M.; Kamaras, K.; Reynolds, J. R.; Tanner, D. B.; Hebard, A. F.;

et al. Transparent, Conductive Carbon Nanotube Films. *Science* **2004,** *305*, 1273–1276.
7. Li, Z. R.; Saini, V.; Dervishi, E.; Kunets, V. P.; Zhang, J. H.; Xu, Y.; Biris, A. R.; Salamo, G. J.; Biris, A. S. Polymer Functionalized n-Type Single Wall Carbon Nanotube Photovoltaic Devices. *Appl. Phys. Lett.* **2010,** 96.
8. Jacobs, C. B.; Peairs, M. J.; Venton, B. J. Review: Carbon Nanotube Based Electrochemical Sensors for Biomolecules. *Anal. Chim. Acta* **2010,** *662*, 105–127.
9. Rowe, D. M. *CRC Handbook of Thermoelectrics*; CRC Press: Boca Raton, FL, 1995.
10. Mahan, G. D.; Sofo, J. O. The Best Thermoelectric. *Proc. Natl. Acad. Sci. U.S.A.* **1996,** *93*, 7436–7439.
11. Qu, L. T.; Dai, L. M. Substrate-Enhanced Electroless Deposition of Metal Nanoparticles on Carbon Nanotubes. *J. Am. Chem. Soc.* **2005,** *127*, 10806–10807.
12. Choi, H. C.; Shim, M.; Bangsaruntip, S.; Dai, H. J. Spontaneous Reduction of Metal Ions on the Sidewalls of Carbon Nanotubes. *J. Am. Chem. Soc.* **2002,** *124*, 9058–9059.
13. http://en.wikipedia.org/wiki/table_of_standard_electrode_potentials.
14. Liu, P.; Sun, Q.; Zhu, F.; Liu, K.; Jiang, K.; Liu, L.; Li, Q.; Fan, S. Measuring the Work Function of Carbon Nanotubes with Thermionic Method. *Nano Lett.* **2008,** *8*, 647–651.
15. Zhao, J. J.; Han, J.; Lu, J. P. Work Functions of Pristine and Alkali-Metal Intercalated Carbon Nanotubes and Bundles. *Phys. Rev. B* **2002,** 65.
16. Collins, P. G.; Bradley, K.; Ishigami, M.; Zettl, A. Extreme Oxygen Sensitivity of Electronic Properties of Carbon Nanotubes. *Science* **2000,** *287*, 1801–1804.
17. Park, J.-H.; Natesant, K. Oxidation of Copper and Electronic Transport in Copper Oxides. *Oxid. Met.* **1993,** *39*, 411–435.
18. Lawless, K. R. The Oxidation of Metals. *Rep. Prog. Phys.* **1974,** *37*, 231–316.
19. http://en.wikipedia.org/wiki/copper.
20. Ebbesen, T. W.; Lezec, H. J.; Hiura, H.; Bennett, J. W.; Ghaemi, H. F.; Thio, T. Electrical Conductivity of Individual Carbon Nanotubes. *Nature* **1996,** *382*, 54–56.
21. Anderson, P. A. The Work Function of Copper. *Phys. Rev.* **1949,** *76*, 388–390.
22. Eastman, D. E. Photoelectric Work Functions of Transition, Rare-Earth, and Noble Metals. *Phys. Rev. B* **1970,** *2*, 1–2.
23. Chen, G. *Nanoscale Energy Transport and Conversion*; Oxford University Press: New York, 2005.
24. Akai, Y.; Saito, S. Electronic Structure, Energetics and Geometric Structure of Carbon Nanotubes: A Density-Functional Study. *Physica E* **2005,** *29*, 555–559.